

## Interplay of antiferromagnetism, ferromagnetism, and superconductivity in $\text{EuFe}_2(\text{As}_{1-x}\text{P}_x)_2$ single crystals

H. S. Jeevan,<sup>1</sup> Deepa Kasinathan,<sup>2</sup> Helge Rosner,<sup>2</sup> and Philipp Gegenwart<sup>1</sup>

<sup>1</sup>*I. Physikalisches Institut, Georg-August-Universität Göttingen, D-37077 Göttingen, Germany*

<sup>2</sup>*Max-Planck-Institut für Chemische Physik fester Stoffe, D-01187 Dresden, Germany*

(Received 8 December 2010; revised manuscript received 9 January 2011; published 22 February 2011)

We report a systematic study of the influence of antiferromagnetic and ferromagnetic phases of  $\text{Eu}^{2+}$  moments on the superconducting phase upon doping the As site by isovalent P, which essentially acts like chemical pressure on  $\text{EuFe}_2\text{As}_2$ . Bulk superconductivity with transition temperatures of 22 and 28 K are observed for  $x = 0.16$  and  $0.20$  samples, respectively. The Eu ions order antiferromagnetically for  $x \leq 0.13$ , while bulk superconductivity coexists with Eu-antiferromagnetism for  $0.13 < x < 0.22$ . In contrast, a crossover is observed for  $x \geq 0.22$  whereupon the Eu ions order ferromagnetically and superconductivity is fully suppressed. Density-functional-theory-based calculations reproduce the observed experimental findings consistently. We discuss in detail the coexistence of superconductivity and magnetism in a tiny region of the phase space and comment on the competition of ferromagnetism and superconductivity in the title compound.

DOI: [10.1103/PhysRevB.83.054511](https://doi.org/10.1103/PhysRevB.83.054511)

PACS number(s): 74.25.Bt, 71.20.Eh, 74.10.+v, 74.25.Jb

The appearance of superconductivity (SC) in the vicinity of a magnetic instability is often related to quantum critical phenomena,<sup>1,2</sup> although only in a few cases have the magnetic excitations which mediate the SC pairing been identified.<sup>3</sup> The discovery of superconductivity upon suppression of magnetism in iron-containing pnictides and chalcogenides has created great interest in the field of condensed matter physics. Among the various members of the iron-containing pnictides are three main family of materials, which show SC transitions upon substitution by a dopant or upon applying external pressure. They are (i) the quaternary “1111” compounds,  $R\text{FeAsO}$ , where  $R$  represents a lanthanide such as La, Ce, Sm, etc.,<sup>4–7</sup> with transition temperatures as high as 56 K; (ii) the ternary  $A\text{Fe}_2\text{As}_2$  ( $A = \text{Ca, Sr, Ba, Eu}$ )<sup>8–11</sup> systems, also known as “122” systems, which exhibit superconductivity up to 38 K; and (iii) the binary chalcogenide “11” systems (e.g., FeSe) with superconducting transition temperatures up to 14 K.<sup>12</sup> In general, the magnetism occurring in the Fe sublattice can be suppressed by doping via two schemes: (i) direct doping of Fe in the FeAs layer by Co, Ni, Rh (electron doping)<sup>13,14</sup> or Ru (isovalent substitution),<sup>15</sup> and (ii) indirect doping on other sites, which includes oxygen by fluorine in the “1111” systems (electron doping),<sup>4</sup> alkaline earth metals by alkaline metals in the “122” systems (hole doping),<sup>8</sup> and arsenic with phosphorus (isovalent substitution).<sup>16,17</sup> Similar to doping, external pressure also facilitates the suppression of Fe magnetism.<sup>18</sup> In the case of rare-earth-based iron pnictides, a second magnetic sublattice, due to the localized  $f$ -moments, comes into play additionally to the Fe sublattice. In general, the rare-earth ions tend to order antiferromagnetically, thereby introducing only a weak coupling between the two sublattices. In this work we concentrate on  $\text{EuFe}_2\text{As}_2$ , the only rare-earth-based member of the “122” family.  $\text{EuFe}_2\text{As}_2$  exhibits a spin density wave (SDW) in the Fe sublattice together with a structural transition at 190 K, and in addition an A-type antiferromagnetic (AF) order at 19 K due to  $\text{Eu}^{2+}$  ions (ferromagnetic layers ordered antiferromagnetically).<sup>19</sup> Superconductivity can be achieved in this system by substituting Eu with K or Na (Refs. 9 and 20), As with P (Ref. 21), and upon application of external

pressure.<sup>18,22</sup> Pressure studies up to 3 GPa on the parent compound have also shown indications of *reentrant* SC, akin to ternary Chevrel phases or rare-earth nickel borocarbides.<sup>18</sup>

Isovalent P doping on the As site in  $\text{EuFe}_2\text{As}_2$  without introducing holes or electrons simulates a scenario generally referred to as “chemical pressure.” While the  $\text{Eu}^{2+}$  moments order antiferromagnetically (A-type) at 19 K in the parent compound, ferromagnetic order at 27 K is found for the end member  $\text{EuFe}_2\text{P}_2$ .<sup>23</sup> In early 2009, Ren and coworkers<sup>21</sup> reported on the coexistence of SC and ferromagnetism (FM) of the  $\text{Eu}^{2+}$  moments in polycrystalline samples of  $\text{EuFe}_2(\text{As}_{0.7}\text{P}_{0.3})_2$ , with a superconducting transition at 26 K, followed by a FM ordering of the  $\text{Eu}^{2+}$  moments at 20 K. Recently, another report<sup>24</sup> also documents the coexistence of SC (at 26 K) and FM (at 18 K) in  $\text{EuFe}_2(\text{As}_{0.73}\text{P}_{0.27})_2$  along with a reentrant behavior below 16 K. On the other, hand systematic studies by Ren and collaborators on Ni doping in  $\text{EuFe}_{2-x}\text{Ni}_x\text{As}_2$  showed only FM ordering of the  $\text{Eu}^{2+}$  moments but no superconductivity.<sup>25</sup> In contrast, superconductivity has been reported upon Ni doping of the Fe site for the other three members of the  $A\text{Fe}_{2-x}\text{Ni}_x\text{As}_2$  ( $A = \text{Ca, Sr, Ba}$ ) family.<sup>14,26–28</sup> Based on these reports, the physical properties of both Ni- and P-doped  $\text{EuFe}_2\text{As}_2$  samples seem to contradict each other in terms of competition or coexistence of FM and SC phases. In this paper, we report on the detailed investigation of the resistivity, magnetization, and specific heat measurements using well-characterized single crystals of  $\text{EuFe}_2(\text{As}_{1-x}\text{P}_x)_2$  and show the presence of bulk superconductivity up to 28 K. Our measurements also prove that in this system the FM ( $\text{Eu}^{2+}$  ions) and SC phases compete with each other, rather than coexist, in contradiction to the claim of Refs. 21 and 24. Bulk SC coexisting with AF  $\text{Eu}^{2+}$  ordering is found only in a very narrow regime of P doping, where the Fe SDW transition has just been suppressed. The systematic study of P doping on single crystals allows us to draw a phase diagram that is complex and rich with five different phases.

A series of single crystals of  $\text{EuFe}_2(\text{As}_{1-x}\text{P}_x)_2$  with a range of P doping were synthesized using the Bridgman method.

Stoichiometric amounts of starting elements (Eu 99.99%, Fe 99.99%, As 99.9999%, and P 99.99%) were taken in an  $\text{Al}_2\text{O}_3$  crucible, which was then sealed in a Ta crucible under argon atmosphere. The sealed crucible was heated at a rate of  $50\text{ }^\circ\text{C}/\text{hour}$  up to  $1300\text{ }^\circ\text{C}$ , kept for 12 hours at the same temperature, and then cooled to  $950\text{ }^\circ\text{C}$  with a cooling rate of  $3\text{ }^\circ\text{C}/\text{hour}$ . We obtained large platelike single crystals using this process with dimensions of  $5 \times 3\text{ mm}^2$  in the  $ab$  plane. In addition to the platelike single crystals, we also found a secondary polycrystalline phase, which was identified as  $\text{Fe}_2\text{P}$ . All the elements and sample handling were carried out inside a glove box filled with Ar atmosphere. The quality of the single crystals was checked using the Laue method, powder x-ray diffraction, and additionally with scanning electron microscopy equipped with energy dispersive x-ray analysis (EDX). For all doping concentrations considered here, the changes in the compositional inhomogeneity are less than 1% on the cleaved surface of the various single crystals. Electrical resistivity and specific heat were measured using a Physical Properties Measurement System (Quantum Design, USA). Magnetic properties were measured using the Superconducting Quantum Interference Device magnetometer procured from Quantum Design. The change of the electronic properties with phosphorus doping has been investigated by angle-resolved photoemission spectroscopy (ARPES) and optical conductivity measurements<sup>29–31</sup> on our single crystals. ARPES measurements indicate that the electronic structure of the phosphorus-doped systems is more three dimensional compared to the parent compound and as well as to the case of electron doping.<sup>29,30</sup> Recent infrared spectroscopy measurements claim evidence for a single nodeless  $s$ -wave superconducting gap for isovalent substitution in contrast to the multigap scenario in carrier-doped systems.<sup>31</sup> In this paper we focus on the interplay of  $\text{Eu}^{2+}$  magnetism on the formation of SC.

The powder diffraction pattern of all the samples can be indexed using the tetragonal  $\text{ThCr}_2\text{Si}_2$  structure type. The variation of the lattice parameters with respect to P content is collected in Table I, wherein the actual P content is given as determined by EDX. Similar to other isovalent substitutions of 122 systems discussed in the literature,<sup>32</sup> phosphorus substitution on the As site leads to a dramatic decrease of FeAs-layer thickness, which indicates that P doping mainly affects the  $c$  lattice parameter. We also observe that the decrease along the tetragonal axis ( $c$  lattice parameter) is more pronounced compared to the changes in the  $ab$  plane (see Table I).

The temperature dependence of the normalized resistivity (with the current measured in the basal  $ab$  plane) is shown in Fig. 1 for the single crystals of  $\text{EuFe}_2(\text{As}_{1-x}\text{P}_x)_2$ . The temperature dependence of the resistivity shows a metallic behavior for the entire doping range. For the parent compound  $\text{EuFe}_2\text{As}_2$ , we observe both the SDW anomaly associated with the structural and magnetic transition of the Fe sublattice<sup>19</sup> at  $190\text{ K}$  ( $T_{\text{SDW}}$ ) and the anomaly at  $19\text{ K}$  ( $T_N$ ) associated with the AF ordering of the  $\text{Eu}^{2+}$  moments. Upon doping with P, for the lowest P content studied here,  $x = 0.12$ , the resistivity decreases linearly with temperature down to  $90\text{ K}$ , whereupon we observe an anomaly which is likely due to the SDW transition. We observe another anomaly around  $20\text{ K}$  which is

TABLE I. Tetragonal lattice parameters (for selected samples at  $300\text{ K}$ ) of  $\text{EuFe}_2(\text{As}_{1-x}\text{P}_x)_2$  crystallizing in the  $\text{ThCr}_2\text{Si}_2$ -type structure as a function of phosphorus substitution ( $x$ ), which is determined by EDX.

$x$	$a$ (Å)	$c$ (Å)
0	3.907	12.114
0.15	3.891	11.948
0.16	3.890	11.930
0.20	3.887	11.890
0.22	3.889	11.877
0.26	3.889	11.870
0.38	3.885	11.774
1	3.816	11.248

likely associated with the A-type AF ordering of the  $\text{Eu}^{2+}$  ions. No further anomalies are observed for this sample. When the P content is increased, the SDW transition is fully suppressed and a sudden drop in the resistivity indicative of a superconducting (SC) transition is observed for  $x = 0.16$  at  $22\text{ K}$  and for  $x = 0.2$  at  $29\text{ K}$ . For  $x = 0.22$ , a sharp drop in the resistivity is observed around  $25\text{ K}$ , but the normalized resistivity does not go to zero. For larger P concentrations,  $x \geq 0.26$ , the SC transition is fully suppressed. Our observations described here are in contradiction to previous reports,<sup>21,24</sup> which evidence

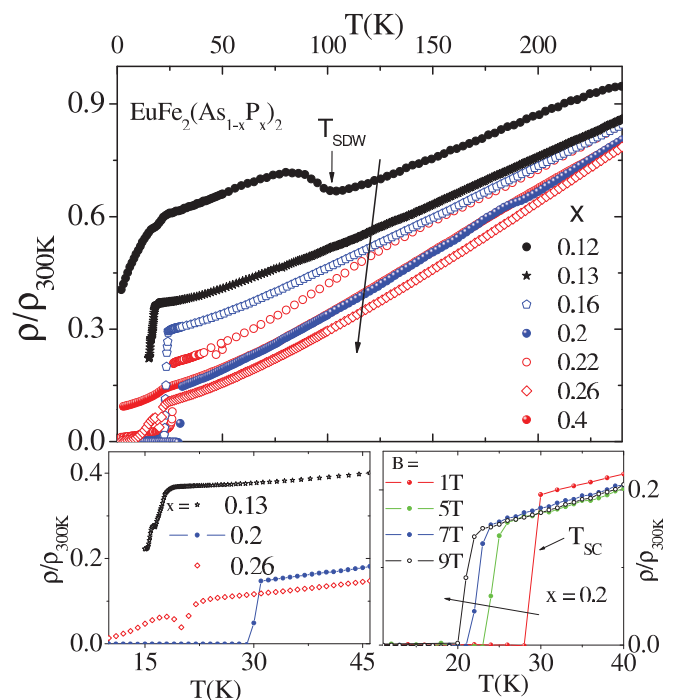


FIG. 1. (Color online) Temperature dependence of the in-plane ( $ab$  plane) resistivity for various  $\text{EuFe}_2(\text{As}_{1-x}\text{P}_x)_2$  single crystals. The data are normalized to the room temperature resistivity. Due to technical reasons, the resistivity for the  $x = 0.13$  sample was measured down to  $15\text{ K}$  only. The lack of SC (zero-resistivity) transition is confirmed by the magnetic susceptibility measurements (Fig. 2). Lower left panel: Low-temperature part of the normalized in-plane resistivity for selected samples. Lower right panel: Normalized in-plane resistivity of the superconducting sample ( $x = 0.2$ ) for various values of the applied magnetic field.

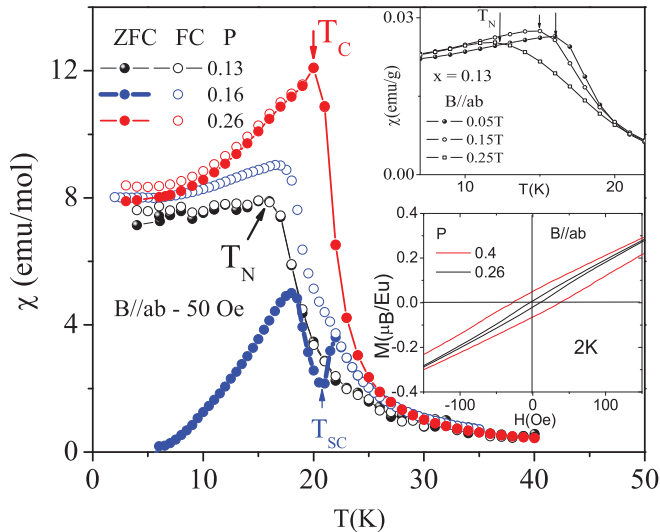


FIG. 2. (Color online) Temperature dependence of the magnetic susceptibility for  $\text{EuFe}_2(\text{As}_{1-x}\text{P}_x)_2$ . Upper inset: Field dependence of the AF transition for the  $x = 0.13$  sample. Lower inset: Isothermal magnetization at 2 K of  $x = 0.26$  and  $0.4$  samples, which show a FM ordering of the  $\text{Eu}^{2+}$  moments.

a SC transition around 26 K for polycrystalline samples with  $x = 0.27$  and  $0.30$ . We do not observe zero resistance consistently for all samples with  $x \geq 0.22$ . The lower right panel of Fig. 1 shows the field dependence of the normalized resistivity of the SC transition temperature for the  $x = 0.2$  sample. The  $\rho(T)/\rho_{300\text{K}}$  shows a sharp drop below 30 K in a zero magnetic field and shifts to lower temperatures as the field increases and reaches 22 K at 9 T, in accordance with the SC properties.

We measured the dc magnetic susceptibility for selected compositions to obtain more insights regarding the nature of the magnetic and SC phases, with the applied magnetic field parallel to the  $ab$  plane. Figure 2 shows the field-cooled (FC) and zero-field-cooled (ZFC) susceptibility at 50 Oe, for  $x = 0.13, 0.16,$  and  $0.26$ . For the underdoped sample ( $x = 0.13$ ) both ZFC and FC data show only the anomaly at 17 K due to AF ordering of the  $\text{Eu}^{2+}$  moments. There are no signs for a SC phase for this sample. For the optimally doped  $x = 0.16$  sample, the susceptibility shows a pronounced diamagnetic step at 22 K, evidence for a bulk SC transition, consistent with the sharp drop observed in resistivity below 22 K. Below 20 K the susceptibility begins to increase and reaches a maximum around 18 K, which is indicative of the AF ordering of the  $\text{Eu}^{2+}$  moments. This observation of the coexistence of SC and AF ordering for  $x = 0.16$  is similar to the ac susceptibility measurements reported previously for the parent compound under 25.7 kbar pressure.<sup>22</sup> Further increasing the P content to  $x = 0.26$ , the magnetic susceptibility shows only an anomaly at 20 K due to the FM ordering of the  $\text{Eu}^{2+}$  moments (discussed later). It is clear from the magnetic susceptibility measurements that bulk SC phase transition is observed only for the  $x = 0.16$  sample, while no sign for a SC phase is inferred for  $x = 0.13$  and  $0.26$  samples. The inset of Fig. 2 shows the field dependence of  $T_N$  for the underdoped sample,  $x = 0.13$ . With increasing fields,  $T_N$  is shifted to lower values. This is indicative of the AF ordering of the  $\text{Eu}^{2+}$  moments.

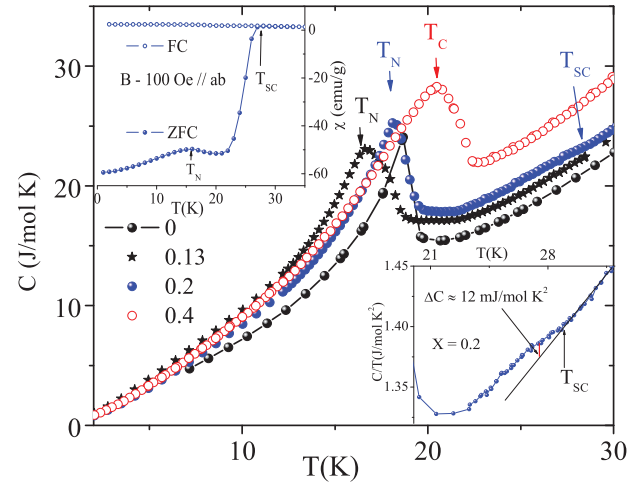


FIG. 3. (Color online) Evolution of AF ( $T_N$ ) and FM ( $T_C$ ) ordering temperatures as a function of phosphorus substitution in the specific heat. Lower inset shows the anomaly of the SC phase transition for the  $x = 0.2$  sample. Upper inset shows the dc magnetic susceptibility for ZFC and FC experiments in applied field of 50 Oe for the  $x = 0.2$  sample.

Upon increasing the P content to  $x = 0.26$ , the Eu ordering changes from AF to FM. The FM ordering of the  $x = 0.26$  and  $0.4$  samples are confirmed by isothermal magnetization measurements at 2 K shown in the lower inset of Fig. 2. A small but clear hysteresis loop is observed as a function of applied field, which is consistent with similar observation in the ferromagnetically ( $T_C = 29$  K) ordered end member  $\text{EuFe}_2\text{P}_2$ .<sup>23</sup> Previous reports<sup>21,24</sup> have claimed the coexistence of SC with FM for  $x = 0.27$  and  $0.3$  polycrystals, which display a tiny ( $10^{-2}$  emu/mol) diamagnetic contribution to the susceptibility together with a broadened resistive transition at 25 K and which also shows a re-entrance behavior around 16 K. The data on single crystals presented here indicate clear bulk SC only within the concentration range  $0.16 \leq 0.2$ . At large P doping, where Eu displays FM ordering, SC appears to be suppressed.

Another confirmation for the bulk nature of the magnetic and SC phases is obtained by measuring the specific heat ( $C_p$ ) in the temperature range from 35 K down to 2 K. The data are collected in Fig. 3 for an underdoped ( $x = 0.13$ ), optimally doped ( $x = 0.2$ ), and overdoped ( $x = 0.4$ ) single crystal. The plot shows clear anomalies for both AFM ( $T_N$ ) and FM ( $T_C$ ) phase transitions for  $x = 0.13$  and  $0.4$ , respectively. Due to strong contributions at low temperatures from the phonons and  $\text{Eu}^{2+}$  magnetic moments to the specific heat, it is difficult to observe an anomaly at the SC phase transition; however, a small anomaly (lower inset of Fig. 3) in the raw data (without subtracting any phonon contribution) is resolved below 28 K for  $x = 0.2$ . This observation is consistent with the diamagnetic step observed in the magnetic susceptibility (upper inset of Fig. 3) as well as the drop in resistivity (Fig. 1). In addition, the magnetic susceptibility for  $x = 0.2$  (ZFC at 50 Oe) shows a small anomaly at 20 K corresponding to the AF transition of the  $\text{Eu}^{2+}$  moments, indicative of a coexistence of AF and SC for this sample. Based on these thermodynamic measurements, we infer that both the magnetism and SC are of

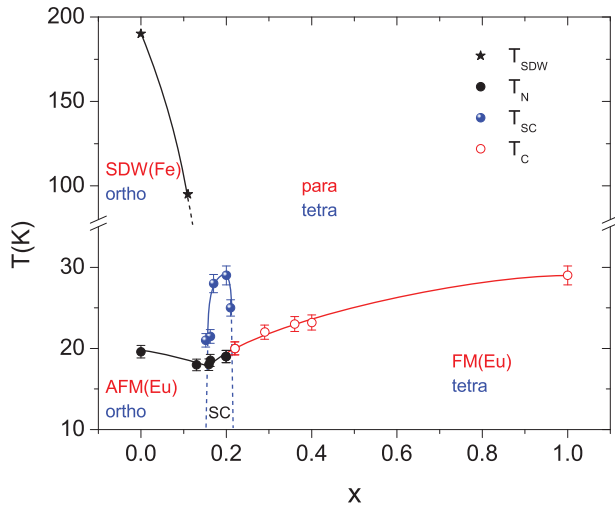


FIG. 4. (Color online) The complex phase diagram for  $\text{EuFe}_2(\text{As}_{1-x}\text{P}_x)_2$  as a function of P. The solid lines act as a guide to the eye, and the dotted lines are extrapolation using the available experimental data in order to complete the superconducting dome.

bulk nature, and furthermore only AF and SC phases coexist for  $\text{EuFe}_2(\text{As}_{1-x}\text{P}_x)_2$ . A single crystal with  $x = 0.18$ , displaying a SC transition at 28 K has also been studied by optical conductivity measurements<sup>31</sup> above and below  $T_C$ . A BCS fit revealed a  $s$ -wave-type gap with  $2\Delta = 3.8k_B T_C$ .

The results obtained from the different measurements allow us to draw the electronic phase diagram of  $\text{EuFe}_2(\text{As}_{1-x}\text{P}_x)_2$  as a function of phosphorus doping. The transition temperatures were determined from specific heat, resistivity, and magnetic susceptibility measurements. Figure 4 shows a complex phase diagram, wherein we have identified five different phases. The parent compound  $\text{EuFe}_2\text{As}_2$  with tetragonal symmetry is paramagnetic at high temperatures (above 190 K), while below 190 K, the structure changes to orthorhombic and the Fe moments order antiferromagnetically (SDW). In addition, below 19 K, the system undergoes another AF transition associated with the  $\text{Eu}^{2+}$  moments. Upon isovalent doping of the As site with P in  $\text{EuFe}_2(\text{As}_{1-x}\text{P}_x)_2$ , for  $0.16 \leq 0.22$  we observe bulk SC phase transitions coexisting with AF ordering of the  $\text{Eu}^{2+}$  moments. Further increasing the P content,  $x \geq 0.26$ , SC is completely suppressed and the  $\text{Eu}^{2+}$  sublattice magnetic interaction changes from AFM to FM. Recently Nandi *et al.* proposed<sup>33</sup> that the coupling between orthorhombicity and superconductivity is indirect and claim that it arises due to the strong competition between magnetism (of Fe) and superconductivity in Co doped  $\text{BaFe}_2\text{As}_2$  systems. This means that the orthorhombic to tetragonal transition occurs at temperatures above the onset of Fe magnetic (SDW) order, and the orthorhombic structure could continue to exist in the superconducting phase too. Similar arguments can be used for the current phase diagram of  $\text{EuFe}_2(\text{As}_{1-x}\text{P}_x)_2$ , where most likely the AF (Eu) and SC phases coexist with the orthorhombic phase. Detailed analysis of the tetragonal-to-orthorhombic distortion on the stability of the FM and AF  $\text{Eu}^{2+}$  sublattice on our samples is in progress. In general, a FM phase is not favorable for SC within  $s$ -wave pairing mechanisms because the Zeeman effect arising due to ferromagnetism will strongly disfavor the singlet formation, which will eventually

lead to the breakdown of the Cooper pairs. FM ordering of  $\text{Eu}^{2+}$  ions will result in an internal magnetic field of reasonable strength due to its large spin value  $S = 7/2$ , which is detrimental to the SC occurring in the FeAs layers. Hence we believe that the previous reports<sup>21,24</sup> on the coexistence of SC and Eu-FM in  $\text{EuFe}_2(\text{As}_{0.73}\text{P}_{0.27})_2$  and  $\text{EuFe}_2(\text{As}_{0.7}\text{P}_{0.3})_2$  might probably be related to inhomogeneous phosphorus-doping concentration in polycrystalline samples.<sup>34</sup> In general, single crystals are compositionally more homogeneous than polycrystalline samples, and the presence of even a few percent volume fraction of the superconducting phase in a given sample should result in a strong drop (not zero) in the resistivity measurements. In our single crystals, with  $x = 0.26$  and  $0.38$ , we did not observe any such drop in resistivity. At this juncture, we would also like to note that, by crushing a single crystal of  $\text{EuFe}_2(\text{As}_{0.62}\text{P}_{0.38})_2$  into a powder, we repeated all our measurements and did not notice any change in our descriptions (i.e., only FM ordering of the  $\text{Eu}^{2+}$  moments was observed, but no SC phase transition).

For a microscopic understanding of the interlayer coupling of the  $\text{Eu}^{2+}$  moments in  $\text{EuFe}_2(\text{As}_{1-x}\text{P}_x)_2$ , we have carried out total energy calculations using the full-potential local orbital code.<sup>35</sup> We used the Perdew-Wang<sup>36</sup> flavor of the exchange-correlation potential, and the energies were converged on a dense  $k$  mesh consisting of  $20^3$  points. The localized Eu 4*f* states were treated on a mean-field level by using the LSDA+*U* (local-spin-density-approximation + strong correlations) approach, applying the so-called “atomic limit” double-counting scheme.<sup>37</sup> In general, the physically relevant value of the strong Coulomb repulsion  $U_{4f}$  of the  $\text{Eu}^{2+}$  ion is inferred from various spectroscopy techniques, especially by photoemission spectroscopy experiments. Owing to the lack of such experiments for  $\text{EuFe}_2\text{As}_2$ , we have therefore used a  $U_{4f}$  value of 7–8 eV.<sup>38</sup> The robustness of our results and consequently the interpretations were checked for consistency with varying  $U_{4f}$  values. The Fe 3*d* states were treated on an itinerant level (LSDA) without additional correlations. The partial P substitution was modeled by the construction of supercells of various sizes. The randomness in possible substitution positions was taken into account by allowing phosphorus to occupy different possible combinations of the fourfold 4*e* As sites. The lattice parameters for the various supercells were obtained by interpolating linearly the experimental data reported in Table I. The As/P  $z$  position was kept fixed at  $z = 0.362$  throughout. Based on density functional theory calculations, we have previously<sup>19</sup> shown that the Eu and Fe sublattices are quite decoupled in  $\text{EuFe}_2\text{As}_2$ . This result is also corroborated experimentally by showing that the  $\text{Eu}^{2+}$  moments play only a minor role in the electronic transport properties.<sup>39</sup> Presently, our goal is to obtain an estimate for the Eu interlayer coupling below  $T_N$  or  $T_C$ , while the Fe sublattice is retained in the SDW pattern. The results from our calculations are collected in Fig. 5. For  $x < 0.2$ , the ground state of  $\text{EuFe}_2(\text{As}_{1-x}\text{P}_x)_2$  is A-type AF, consistent with the above mentioned experimental results. The energy difference between the AF (ground state) and FM alignment of the  $\text{Eu}^{2+}$  moments is quite small (0–6 meV per formula unit). This implies a rather weak interlayer coupling for the Eu sublattice. Any small external effects (impurities, doping, external pressure, and fields) can easily flip the Eu spins from

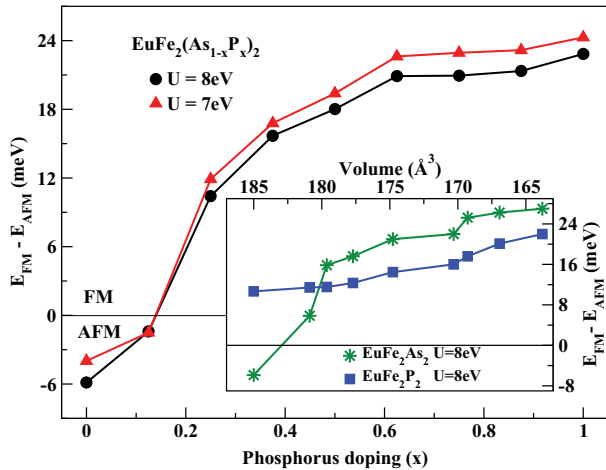


FIG. 5. (Color online) Energy difference between FM- and AF-aligned  $\text{Eu}^{2+}$  moments along the  $c$  axis, as a function of phosphorus content in  $\text{EuFe}_2(\text{As}_{1-x}\text{P}_x)_2$ . Along the  $y$  axis, the ground state is AFM below zero and FM above zero. Inset: Energy difference (same as main panel) as a function of reduced volume for the two end members  $\text{EuFe}_2\text{As}_2$  and  $\text{EuFe}_2\text{P}_2$ . The data points in the inset and the main panel have a one-to-one correspondence.

AF to FM. This has also been shown experimentally by Xiao and co-workers<sup>40</sup> for the parent compound  $\text{EuFe}_2\text{As}_2$ , wherein below  $T_N$  they observe a field-induced spin reorientation to the FM state for an applied field of just 1 T in the  $ab$  plane and at 2 T along the  $c$  axis. For  $x > 0.2$ , FM interlayer coupling between the  $\text{Eu}^{2+}$  moments becomes favorable (i.e., the ground state is FM) and continues to remain so for larger P substitutions, consistent with the present experimental observations. The Fe sublattice remains magnetic for  $0 \leq x \leq 0.875$  with a slight reduction of the individual magnetic moments with increasing phosphorus content. The Fe sublattice becomes nonmagnetic for the end member of this substitution series  $\text{EuFe}_2\text{P}_2$ , while the rare-earth Eu remains divalent in the entire substitution range. These results are also consistent with the recently reported experimental findings of Feng and co-workers<sup>23</sup> for  $\text{EuFe}_2\text{P}_2$ . Another recent report by Sun and collaborators<sup>41</sup> witnessed a valence change of europium from a 2+ to a 3+ state in  $\text{EuFe}_2\text{As}_{1.4}\text{P}_{0.6}$  at ambient conditions along with a SC transition at 19.4 K. They also suggest that the FeAs layers receive the additional charges arising from this valence transition, which in turn steers the onset of SC. This valence change behavior seems rather counterintuitive, since the end member  $\text{EuFe}_2\text{P}_2$  is a well-known ferromagnet with divalent europium.<sup>42</sup> One should also note that other alkaline-earth-based members of the “122” family have been shown to superconduct upon isovalent doping either on the Fe site or on the As site, without the possibility of additional charges entering the FeAs layers.<sup>14,15,26–28</sup> LDA+ $U$  calculations favor integer occupation, but a qualitative description of the valence transitions can be obtained from such calculations.<sup>43</sup> Therefore, we investigated the possibility of such a valence change ( $\text{Eu}^{2+} \rightarrow \text{Eu}^{3+}$ ) in our calculations and found that europium always favors the divalent state in the entire substitution range.

As mentioned earlier, without the introduction of additional holes or electrons, isovalent doping of As by P introduces

“chemical pressure” in  $\text{EuFe}_2(\text{As}_{1-x}\text{P}_x)_2$ . The phosphorus ion is smaller than the arsenic ion, and the lattice parameters shrink rather anisotropically ( $c/a$  decreases significantly) with increasing phosphorus content (see Table I), and the lattice becomes more three-dimensional. Similar anisotropic changes to the lattice parameters along with a strong decrease of the  $c/a$  ratio leading to bulk SC were also observed for isovalent substitution of Fe by larger Ru atoms.<sup>15</sup> The substitution of As by P and as well as the decrease in the volume of the unit cell together influence the magnetism of the Eu sublattice. In order to decouple these two effects, substitution and volume reduction, and henceforth obtain a deeper understanding of the chemistry and lattice effects, respectively, we performed two further calculations: (i) parent compound  $\text{EuFe}_2\text{As}_2$  as a function of reduced volume and (ii) end member  $\text{EuFe}_2\text{P}_2$  as a function of expanded volume. The previously described supercell calculations provide information on the effects of substitution, while the current calculations explain the effects of the lattice. Our findings are summarized in the inset of Fig. 5. The data points in the inset have a one-to-one correspondence with the doping ( $x$ ) values in the main panel. The ground state of  $\text{EuFe}_2\text{As}_2$  changes from AF to FM earlier than that of  $\text{EuFe}_2(\text{As}_{1-x}\text{P}_x)_2$ . The As  $4p$  states are more extended than P  $3p$  states, which when combined with a strong decrease of the  $c$  axis tends to influence the interlayer magnetic interaction of the  $\text{Eu}^{2+}$  ions more than phosphorus. On the contrary,  $\text{Eu}^{2+}$  moments in  $\text{EuFe}_2\text{P}_2$  remain FM for all volumes in our calculations. The reported ambient conditions volume from experiments for  $\text{EuFe}_2\text{P}_2$  is  $163.79 \text{ \AA}^3$  (Ref. 23) with FM-aligned Eu ions. Expanding this lattice to  $185 \text{ \AA}^3$  (room-temperature volume of  $\text{EuFe}_2\text{As}_2$ ) reduces the strength of the FM interaction between the interlayer Eu ions but does not flip the spins. Combining these results, we infer that the lattice effects play the major role in influencing the interplay of Eu magnetism in  $\text{EuFe}_2(\text{As}_{1-x}\text{P}_x)_2$ . Similar to the described “chemical pressure” scenario in the title compound, one can concurrently infer that lattice effects (compression of the unit cell) are equally significant to the observation of SC upon application of external “physical” pressure in all the parent 122 systems.<sup>18,44,45</sup>

In summary, we have systematically grown high-quality single crystals and studied the transport, magnetic, and thermodynamic properties on a series of  $\text{EuFe}_2(\text{As}_{1-x}\text{P}_x)_2$  samples, and we have explored the details of the interplay of AF and FM phase of  $\text{Eu}^{2+}$  moments with the SC phase as a function of phosphorus doping. We find that the SDW transition associated with the Fe moments can be suppressed upon P doping, and we have obtained a bulk SC phase transition up to 28 K for  $x = 0.2$ . Further increasing the P content, SC vanishes and  $\text{Eu}^{2+}$  ordering changes from AF to FM. Our results suggest that SC and FM phases compete with each other. Careful analysis also shows that the bulk SC phase coexists with Eu AF phase, possibly in orthorhombic symmetry. Density-functional-theory-based calculations also witness a change in the ordering of the  $\text{Eu}^{2+}$  moments from AF to FM with increasing phosphorus content. Further analysis allows us to infer that the lattice effects are more conducive to the AF to FM transformation of the  $\text{Eu}^{2+}$  moments, rather than the phosphorus substitution itself. More microscopic experiments such as

$\mu$ SR, low-temperature powder diffraction, NMR, etc., are currently in progress to confirm the different phases reported here.

The authors would like to thank C. Geibel, Y. Tokiwa, and K. Winzer for discussion and help. We acknowledge financial support by the DFG Research Unit SPP-1458.

- 
- <sup>1</sup>N. D. Mathur, F. M. Grosche, S. R. Julian, I. R. Walker, D. M. Freye, R. K. W. Haselwimmer, and G. G. Lonzarich, *Nature (London)* **394**, 39 (1998).
- <sup>2</sup>O. Stockert *et al.*, *Phys. Rev. Lett.* **92**, 136401 (2004).
- <sup>3</sup>N. K. Sato, N. Aso, K. Miyake, R. Shiina, P. Thalmeier, G. Varelogiannis, C. Geibel, F. Steglich, P. Fulde, and T. Komatsubara, *Nature (London)* **410**, 340 (2001).
- <sup>4</sup>Y. Kamihara, T. Watanabe, M. Hirano, and H. Hosono, *J. Am. Chem. Soc.* **130**, 3296 (2008).
- <sup>5</sup>H. Takahashi, K. Igawa, K. Arii, Y. Kamihara, M. Hirano, and H. Hosono, *Nature (London)* **453**, 376 (2008).
- <sup>6</sup>X. H. Chen, T. Wu, G. Wu, R. H. Liu, H. Chen, and D. F. Fang, *Nature (London)* **453**, 761 (2008).
- <sup>7</sup>G. F. Chen, Z. Li, D. Wu, G. Li, W. Z. Hu, J. Dong, P. Zheng, J. L. Luo, and N. L. Wang, *Phys. Rev. Lett.* **100**, 247002 (2008).
- <sup>8</sup>M. Rotter, M. Tegel, and D. Johrendt, *Phys. Rev. Lett.* **101**, 107006 (2008).
- <sup>9</sup>H. S. Jeevan, Z. Hossain, D. Kasinathan, H. Rosner, C. Geibel, and P. Gegenwart, *Phys. Rev. B* **78**, 092406 (2008).
- <sup>10</sup>K. Sasmal, B. Lv, B. Lorenz, A. M. Guloy, F. Chen, Y. Y. Xue, and C. W. Chu, *Phys. Rev. Lett.* **101**, 107007 (2008).
- <sup>11</sup>G. Wu, H. Chen, T. Wu, Y. L. Xie, Y. J. Yan, R. H. Liu, X. F. Wang, J. J. Ying, and X. H. Chen, *J. Phys. Condens. Matter* **20**, 422201 (2008).
- <sup>12</sup>F. C. Hsu *et al.*, *Proc. Natl. Acad. Sci. USA.* **105**, 14262 (2008).
- <sup>13</sup>A. Leithe-Jasper, W. Schnelle, C. Geibel, and H. Rosner, *Phys. Rev. Lett.* **101**, 207004 (2008).
- <sup>14</sup>D. Kasinathan, A. Ormeci, K. Koch, U. Burkhardt, W. Schnelle, A. Leithe-Jasper, and H. Rosner, *New J. Phys.* **11**, 025023 (2009).
- <sup>15</sup>W. Schnelle, A. Leithe-Jasper, R. Gumeniuk, U. Burkhardt, D. Kasinathan, and H. Rosner, *Phys. Rev. B* **79**, 214516 (2009).
- <sup>16</sup>C. Wang, S. Jiang, Q. Tao, Z. Ren, Y. Li, L. Li, C. Feng, J. Dai, G. Cao, and Z. Xu, *Eur. Phys. Lett.* **86**, 47002 (2009).
- <sup>17</sup>S. Jiang, H. Xing, G. Xuan, C. Wang, Z. Ren, C. Feng, J. Dai, Z. Xu, and G. Cao, *J. Phys. Condens. Matter* **21**, 382203 (2009).
- <sup>18</sup>C. F. Miclea, M. Nicklas, H. S. Jeevan, D. Kasinathan, Z. Hossain, H. Rosner, P. Gegenwart, C. Geibel, and F. Steglich, *Phys. Rev. B* **79**, 212509 (2009).
- <sup>19</sup>H. S. Jeevan, Z. Hossain, D. Kasinathan, H. Rosner, C. Geibel, and P. Gegenwart, *Phys. Rev. B* **78**, 052502 (2008).
- <sup>20</sup>Y. Qi, Z. Gao, L. Wang, D. Wang, X. Zhang, and Y. Ma, *New J. Phys.* **10**, 123003 (2008).
- <sup>21</sup>Z. Ren, Q. Tao, S. Jiang, C. Feng, C. Wang, J. Dai, G. Cao, and Z. Xu, *Phys. Rev. Lett.* **102**, 137002 (2009).
- <sup>22</sup>T. Terashima *et al.*, *J. Phys. Soc. Jpn.* **78**, 083701 (2009).
- <sup>23</sup>C. Feng, Z. Ren, S. Xu, Z. Xu, G. Cao, I. Nowik, I. Felner, K. Matsubayashi, and Y. Uwatoko, *Phys. Rev. B* **82**, 094426 (2010).
- <sup>24</sup>A. Ahmed, M. Itou, S. Xu, Z. Xu, G. Cao, Y. Sakurai, J. Penner-Hahn, and A. Deb, *Phys. Rev. Lett.* **105**, 207003 (2010).
- <sup>25</sup>Z. Ren, X. Lin, Q. Tao, S. Jiang, Z. Zhu, C. Wang, G. Cao, and Z. Xu, *Phys. Rev. B* **79**, 094426 (2009).
- <sup>26</sup>S. R. Saha, N. P. Butch, K. Kirshenbaum, and J. Paglione, *Phys. Rev. B* **79**, 224519 (2009).
- <sup>27</sup>L. J. Li *et al.*, *New J. Phys.* **11**, 025008 (2009).
- <sup>28</sup>N. Kumar, S. Chi, Y. Chen, K. G. Rana, A. K. Nigam, A. Thamizhavel, W. Ratcliff II, S. K. Dhar, and J. W. Lynn, *Phys. Rev. B* **80**, 144524 (2009).
- <sup>29</sup>S. Thirupathaiah *et al.*, e-print [arXiv:1007.5205](https://arxiv.org/abs/1007.5205).
- <sup>30</sup>L. Rettig, R. Corts, S. Thirupathaiah, P. Gegenwart, H. S. Jeevan, T. Wolf, U. Bovensiepen, M. Wolf, H. A. Drr, J. Fink, e-print [arXiv:1008.1561](https://arxiv.org/abs/1008.1561).
- <sup>31</sup>D. Wu, G. Chanda, H. S. Jeevan, P. Gegenwart, M. Dressel, *Phys. Rev. B (Rapid)* in Press.
- <sup>32</sup>S. Jiang, H. Xing, G. Xuan, C. Wang, Z. Ren, C. Feng, J. Dai, Z. Xu, G. Cao, *J. Phys. Condens. Matter* **21**, 382203 (2009).
- <sup>33</sup>S. Nandi *et al.*, *Phys. Rev. Lett.* **104**, 057006 (2010).
- <sup>34</sup>Note that in Ref. 24, despite the coexistence of SC and Eu-FM order, a competition of SC and Fe-FM was claimed.
- <sup>35</sup>K. Koepf and H. Eschrig, *Phys. Rev. B* **59**, 1743 (1999).
- <sup>36</sup>J. P. Perdew and Y. Wang, *Phys. Rev. B* **45**, 13244 (1992).
- <sup>37</sup>M. T. Czyżyk and G. A. Sawatzky, *Phys. Rev. B* **49**, 14211 (1994).
- <sup>38</sup>Another way of obtaining an estimate for “ $U$ ” is the energy difference of the spectral weight transfer due to a valence change of Eu from a 2+ to a 3+ state. A recent report (Ref. 41) evidences such a valence transition under pressure for  $\text{EuFe}_2\text{As}_2$ , and consistent with our assumptions for “ $U_{4f}$ ,” the energy difference between the main  $\text{Eu}^{2+}$  peak and the satellite  $\text{Eu}^{3+}$  peak is  $\approx 8$  eV.
- <sup>39</sup>T. Terashima, N. Kurita, A. Kikkawa, H. S. Suzuki, T. Matsumoto, K. Murata, and S. Uji, *J. Phys. Soc. Jpn.* **79**, 103706 (2010).
- <sup>40</sup>Y. Xiao *et al.*, *Phys. Rev. B* **81**, 220406 (2010).
- <sup>41</sup>L. Sun *et al.*, *Phys. Rev. B* **82**, 134509 (2010).
- <sup>42</sup>E. Mörsen, B. D. Mosel, W. Müller Warmuth, M. Reehuis, and W. Jeitschko, *J. Phys. Chem. Solids* **49**, 785 (1988).
- <sup>43</sup>R. Gumeniuk, M. Schmitt, C. Loison, W. Carrillo-Cabrera, U. Burkhardt, G. Auffermann, M. Schmidt, W. Schnelle, C. Geibel, A. Leithe-Jasper, and H. Rosner, *Phys. Rev. B* **82**, 235113 (2010).
- <sup>44</sup>M. S. Torikachvili, S. L. Bud’ko, N. Ni, and P. C. Canfield, *Phys. Rev. Lett.* **101**, 057006 (2008).
- <sup>45</sup>P. L. Alireza, Y. T. Chris Ko, J. Gillett, C. M. Petrone, J. M. Cole, S. E. Sebastian, and G. G. Lonzarich, *J. Phys. Condens. Matter* **21**, 012208 (2008).